APPLIED AND ENVIRONMENTAL MICROBIOLOGY, Mar. 2005, p. 1570–1580 Vol. 71, No. 3
0099-2240/05/$08.00+0 doi:10.1128/AEM.71.3.1570–1580.2005

Subtle Difference between Benzene and Toluene Dioxygenases of *Pseudomonas putida*

Claire Bagnéris,* Richard Cammack, and Jeremy R. Mason

Molecular Genetics and Microbiology Group, Division of Life Sciences, King's College London, London, United Kingdom

Received 13 July 2004/Accepted 6 October 2004

Benzene dioxygenase and toluene dioxygenase from *Pseudomonas putida* have similar catalytic properties, structures, and gene organizations, but they differ in substrate specificity, with toluene dioxygenase having higher activity toward alkylbenzenes. The catalytic iron-sulfur proteins of these enzymes consist of two dissimilar subunits, α and β; the α subunit contains a [2Fe-2S] cluster involved in electron transfer, the catalytic nonheme iron center, and is also responsible for substrate specificity. The amino acid sequences of the α subunits of benzene and toluene dioxygenases differ at only 33 of 450 amino acids. Chimeric proteins and mutants of the benzene dioxygenase α subunit were constructed to determine which of these residues were primarily responsible for the change in specificity. The protein containing toluene dioxygenase C-terminal region residues 281 to 363 showed greater substrate preference for alkyl benzenes. In addition, we identified four amino acid substitutions in this region, I301V, T305S, I307L, and L309V, that particularly enhanced the preference for ethylbenzene. The positions of these amino acids in the α subunit structure were modeled by comparison with the crystal structure of naphthalene dioxygenase. They were not in the substrate-binding pocket but were adjacent to residues that lined the channel through which substrates were predicted to enter the active site. However, the quadruple mutant also showed a high uncoupled rate of electron transfer without product formation. Finally, the modified proteins showed altered patterns of products formed from toluene and ethylbenzene, including monohydroxylated side chains. We propose that these properties can be explained by a more facile diffusion of the substrate in and out of the substrate cavity.

The ring-hydroxylating dioxygenases of prokaryotes are nonheme iron enzymes that convert aromatic compounds to dihydrodiols in the presence of dioxygen and NADH (6). They act upon a wide range of compounds, which the organisms use as carbon and energy sources. The enzymes are important in the bioremediation of environmental pollutants. Although none of them is completely specific, the dioxygenases display selectivity for the compounds that they metabolize. Moreover, they convert these substrates into stereo- and regiospecific products. These properties make them valuable in the enantio-controlled synthesis of compounds (21).

The benzene 1,2-dioxygenase from *Pseudomonas putida* ML2 (EC 1.14.12.3) is an extensively studied enzyme system (6, 33, 35, 44) that catalyzes the dihydroxylation of benzene to (1*R*,2*S*)-*cis*-cyclohexa-3,5-diene-1,2-diol (benzene *cis*-dihydrodiol), the first step in biodegradation of this xenobiotic compound. The enzyme system has three components: a flavoprotein reductase and a ferredoxin, which transfer electrons from NADH, and a catalytic iron-sulfur protein (ISP_{BED}). ISP_{BED} contains a Rieske-type [2Fe-2S] cluster, a mononuclear nonheme iron oxygen activation center, and a substrate-binding site (6, 22, 25). The ISP_{BED} component comprises two dissimilar subunits, $ISP_{BED}\alpha$ and $ISP_{BED}\beta$ (55). A closely related enzyme that preferentially metabolized ethylbenzene and toluene, toluene dioxygenase ISP_{TOD} (EC 1.14.12.11), was isolated from *P. putida* F1 (13). Much evidence has accumulated that the α subunit of the ISP contains the region that confers substrate specificity (2, 3, 5, 8, 9, 17, 26, 34, 36–38, 47). The genes encoding benzene and toluene dioxygenase systems have been cloned, sequenced, and expressed separately and in combination in *Escherichia coli* (35, 49, 50, 57, 58), but the molecular structures of the enzymes have not been determined. However several structures are now available for the naphthalene dioxygenase ISP (25), which has a homologous amino acid sequence (35.2% identity with ISP_{BED}) (24). The enzyme comprises a trimeric arrangement of two types of subunits, $\alpha_3\beta_3$.

The manipulation of enzyme specificity, both for the substrates used and for the products formed, is important for biotechnology. It is necessary to minimize undesirable side reactions, such as the generation of products that cannot be metabolized or the direct oxidation of NADH without substrate oxidation (the uncoupling reaction). Enzymes that are isolated from the natural environment have been optimized by evolution to avoid these difficulties. To better design new enzymes, it is worthwhile to examine naturally occurring enzymes with different specificities in order to determine which features of the sequence are necessary for efficient and specific catalysis.

Alignment of the nucleotide and amino acid sequences of $ISP_{BED}\alpha$ (50) and $ISP_{TOD}\alpha$ (57) revealed that they differ by 33 amino acids, distributed through the sequence. The first objective of this study was to investigate which of these amino acid differences is necessary for conversion of the substrate preference of benzene dioxygenase from benzene to alkyl-substituted aromatic hydrocarbons, such as toluene and ethylbenzene. The N- and C-terminal domains of toluene and benzene dioxygenases were interchanged, and then individual amino acids were

* Corresponding author. Present address: School of Crystallography, Birkbeck College, University of London, Bloomsbury, Malet St., London WC1E 7HX, United Kingdom. Phone: 44 20 7631 6807. Fax: 44 20 7631 6803. E-mail: c.bagneris@mail.cryst.bbk.ac.uk.

mutated. The recombinant proteins were subcloned and expressed in an isogenic background in *E. coli*. The properties of the variant enzymes were investigated by examining the activities with benzene, toluene, and ethylbenzene by an oxygen electrode assay and by performing product formation assays with radiolabeled substrates, TLC, and GC-MS.

MATERIALS AND METHODS

Abbreviations. GC-MS, gas-chromatography-mass spectrometry; TLC, thin-layer chromatography; SDS, sodium dodecyl sulfate; PAGE, polyacrylamide gel electrophoresis; ISP, iron-sulfur protein of terminal dioxygenase; $ISP_{BED}\alpha$ and $ISP_{TOD}\alpha$, iron-sulfur proteins of benzene and toluene dioxygenases, respectively; $ISP_{BOD}\alpha$ and $ISP_{TED}\alpha$, chimeric α subunits with N-terminal regions from benzene and toluene dioxygenases and C-terminal regions from toluene and benzene dioxygenases, respectively; $ISP_{BOD2}\alpha$, $ISP_{BED}\alpha$ with residues 364 to 450 of $ISP_{TOD}\alpha$; $ISP_{BOD3}\alpha$, $ISP_{BED}\alpha$ with residues 281 to 363 of $ISP_{TOD}\alpha$.

Bacterial strains and plasmids. Bacterial strains and plasmids used in this study are listed in Table 1. *E. coli* JM109 was used for standard cloning and gene expression. *E. coli* CJ236 was used in the mutagenesis experiment with uracil-containing DNA. Transformations were carried out by the method of Hanahan (16).

Cloning strategies. To construct $ISP_{BOD}\alpha$ encoded by plasmid pJRM5041 (Fig. 1A), the EcoRI-BstEII fragment from pJRM504 encoding $ISP_{BED}\alpha$ (residues 1 to 280) was ligated to the BstEII-HindIII fragment (residues 281 to 450) from pSA109 encoding $ISP_{TOD}\alpha$. $ISP_{TED}\alpha$ encoded by plasmid pCMB101 was constructed by ligating the EcoRI-BstEII fragment from pSA109 with the BstEII-HindIII fragment from pJRM504. The two constructs that had the 5′ end from plasmid pSA109 had a lower expression level due to a difference of nine nucleotides with a high adenosine content in the ribosome-binding domain (45). To increase the level of expression, this sequence (CCAAAAAGT) was introduced into the Shine-Dalgarno sequence by carrying out PCR with pSA109 by using forward primer KPIf, which contained the 9-nucleotide sequence and a KpnI restriction site, and reverse primer BEIIr, which contained a BstEII restriction site. The positions of the primers are shown in Table 2. PCRs were carried out for 25 cycles of denaturation at 94°C for 20 s, primer annealing at 55°C for 20 s, and primer extension at 74°C for 60 s. The amplified DNA was digested with KpnI and BstEII and ligated into the BstEII-KpnI fragment of pJRM504 to construct pJRM5043 ($ISP_{TED}\alpha$ modified). Plasmid pJRM5042, containing $ISP_{TOD}\alpha$ modified in the Shine-Dalgarno region, was constructed by ligation of the pJRM5043 HindIII-BstEII fragment with the BstEII-HindIII fragment of pSA109 (Fig. 1A).

Two chimeric ISP α subunits in the C-terminal region, $ISP_{BOD2}\alpha$ and $ISP_{BOD3}\alpha$, were generated by using an approach similar to the approach described above (Fig. 1A). $ISP_{BOD2}\alpha$ contained the N-terminal region of $ISP_{BED}\alpha$ (residues 1 to 363) linked to the SnaBI-HindIII C-terminal region of $ISP_{TOD}\alpha$ (residues 364 to 450). $ISP_{BOD3}\alpha$ was $ISP_{BED}\alpha$ with the BstEII-SnaBI region (residues 281 to 363) replaced with the BstEII-SnaBI region of $ISP_{TOD}\alpha$.

To construct the coexpression vectors encoding $ISP_{TOD}\alpha$-$ISP_{BED}\beta$ and $ISP_{BOD}\alpha$-$ISP_{BED}\beta$, PCRs were carried out with plasmids pJRM5042 (encoding $ISP_{TOD}\alpha$) and pJRM5041 (encoding $ISP_{BOD}\alpha$), respectively, by using primers PKKf and AGIr (Table 2). The PCR products were digested with EcoRI and AgeI and ligated into pJRM502 (encoding $ISP_{BED}\alpha$-$ISP_{BED}\beta$) previously digested with the same enzymes to construct plasmids pJRM502-1 and pJRM502-2, respectively. The correct clones were selected by restriction analysis and DNA sequencing.

Mutagenesis. Site-directed mutagenesis was performed by using both the uracil-containing DNA-based mutagenesis method developed by Kunkel (27) and a PCR-based mutagenesis method adapted from the method of Kammann et al. (23). For uracil-containing DNA-based mutagenesis, plasmid pCB1 containing an F1 origin and encoding $ISP_{BED}\alpha$ was transformed into *E. coli* strain CJ236 (*ung dut*). After production of single-stranded DNA with the VCM13 helper phage (Stratagene), mutagenesis was carried out with a Muta-gene kit (Bio-Rad). The mutated DNA was further cloned into expression vector pJRM504 ($ISP_{BED}\alpha$). For PCR-based mutagenesis, the first PCR was carried out with the wild-type $ISP_{BED}\alpha$ gene (plasmid pJRM504) by using the mutant oligonucleotide and a nonmutagenic oligonucleotide facing in the opposite direction at a distance of about 100 bp. The product was then used as a megaoligonucleotide in a second PCR with another nonmutagenic oligonucleotide facing in the opposite direction at a distance of about 250 bp. The final product was digested and ligated into the wild-type $ISP_{BED}\alpha$ gene. The mutagenic oligonucleotides were designed with a silent mutation that generated a new restriction site (Table 2) to facilitate identification of clones carrying the desired mutation. Successful mutations were identified by restriction analysis and DNA sequencing.

TABLE 1. Bacterial strains and plasmids used in this study

Strain or plasmid	Relevant characteristics
Strains	
E. coli JM109[a]	*endA1 recA1 gyrA96 thi hsdR17 relA1 supE44* Δ(*lac-proAB*) [F′ *traD36 proAB lacI*^{q} *Z*ΔM15]
E. coli CJ236[b]	*dut-1 ung-1 thi-1 rela1* F′ pCJ105 (Cm^r)
Plasmids	
pGEM 3Zf(+)	P_{lac} *lacZ* Amp^r
pKK223-3	P_{lac} Amp^r
pCB1[c]	1.6-kb DraI/EcoRI *bedC1* insert in pGEM 3Zf(+)
pJRM502[c]	2-kb EcoRI/Pst1 *bedC1C2* insert in pKK223-3
pJRM502-1	2-kb EcoRI/PstI *todC1-bedC2* insert in pKK223-3
pJRM502-2	2-kb EcoRI/PstI *bodC1-bedC2* insert in pKK223-3
pJRM503[d]	1.7-kb EcoRI *bedBA* insert in pKK223-3
pJRM504[c]	1.6-kb EcoRI/HindIII *bedC1* insert in pKK223-3
pJRM505[d]	0.7-kb EcoRI/PstI *bedC2* insert in pKK223-3
pJRM711	0.66-kb EcoRI *todC2* insert in pKK223-3
pSA109[d]	1.6-kb EcoRI/PstI *todC1* insert in pKK223-3
pJRM5042	1.6-kb EcoRI/PstI *todC1* modified insert in pKK223-3
pJRM5041	1.6-kb EcoRI/PstI *bodC1* insert in pKK223-3
pJRM5041-1	1.6-kb EcoRI/HindIII *bod2C1* insert in pKK223-3
pJRM5041-2	1.6-kb EcoRI/HindIII *bod3C1* insert in pKK223-3
pCMB101	1.6-kb EcoRI/PstI *tedC1* insert in pKK223-3
pJRM5043	1.6-kb EcoRI/HindIII *tedC1* modified insert in pKK223-3
pCB1M1	pCB1 (L285W)
pCB1M2	pCB1 (A291S)
pCB1M3	pCB1 (L285W/A291S)
pCB1M5	pCB1 (V324I/I327V)
pCB1M7	pCB1 (G404D)
pCB1M9	pCB1 (K436R)
pJRM504M1	pJRM504(L285W)
pJRM504M2	pJRM504(A291S)
pJRM504M3	pJRM504(L285W/A291S)
pJRM504M4[e]	pJRM504(I301V/T305S/I307L/L309V)
pJRM504M5	pJRM504(V324I/I327V)
pJRM504M6[e]	pJRM504(L285W/A291S/G404D)
pJRM504M7	pJRM504(G404D)
pJRM504M8[e]	pJRM504(I412V)
pJRM504M9	pJRM504(K436R)
pJRM504M10[e]	pJRM504(E444D)

[a] See reference 54.
[b] Obtained from Bio-Rad.
[c] Gift of C. S. Butler.
[d] Gift of S. Anguravirutt.
[e] Mutant $ISP_{BED}\alpha$ generated by PCR-based mutagenesis.

Expression of the genes in *E. coli* JM109 and preparation of cell extracts. Cultures of *E. coli* JM109 cells carrying the different plasmids were grown at 37°C in L broth containing ampicillin (100 μg ml^{-1}) to an optical density at 660 nm of 0.7 and then were grown at 30°C after induction with 1 mM isopropyl-β-D-thiogalactopyranoside (IPTG). The cells were harvested in the late exponential

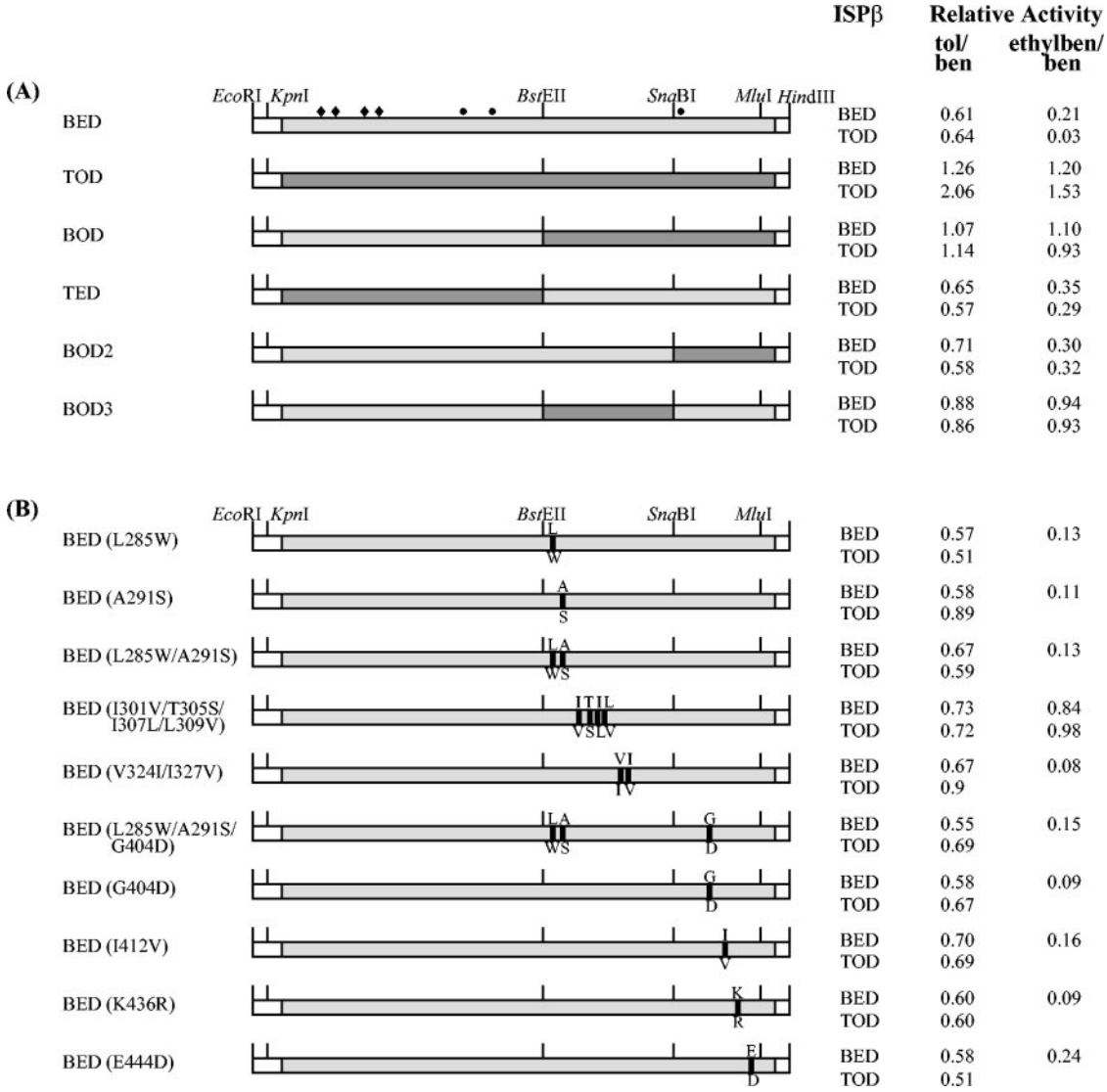

FIG. 1. (A) Diagram of the genes encoding $ISP_{BED}\alpha$, $ISP_{TOD}\alpha$, $ISP_{BOD}\alpha$, $ISP_{TED}\alpha$, $ISP_{BOD2}\alpha$, and $ISP_{BOD3}\alpha$ and relative activities of the corresponding cell extracts. (B) Diagram of the single and multiple mutations created in the $ISP_{BED}\alpha$ C-terminal region and the effects of the mutations on the relative activity. The bars indicate the open reading frames encoding ISP α subunit proteins. The nonconserved amino acids targeted for mutation are indicated by solid boxes. The letters above the bars indicate translated amino acids in $ISP_{BED}\alpha$, and the letters below the bars indicate amino acids in $ISP_{TOD}\alpha$. The numbering corresponds to the numbering for the amino acids in the $ISP_{BED}\alpha$ sequence. Solid diamonds indicate the conserved histidine (H98 and H119) and cysteine (C96 and C116) residues responsible for coordination of the [2Fe-2S] cluster. Solid circles indicate the conserved amino acids (two histidines [H222 and H228] and one aspartate [D376]) involved in coordination of the nonheme iron. The EcoRI, KpnI, BstEII, SnaBI, MluI, and HindIII sites are the restriction sites used for cloning the recombinant α subunit genes. The relative activities with toluene (tol) and ethylbenzene (ethylben) are compared to the activity with benzene (ben), and the data are based on the rate of O_2 uptake measured polarographically by using ISP_{BED} or ISP_{TOD} β subunits, as described in Materials and Methods (means of three determinations).

phase, washed once in 50 mM potassium phosphate (pH 7.2), and resuspended in 25 mM potassium phosphate (pH 7.2)–1 mM dithiothreitol (2 ml/g [wet weight]). The cells were disrupted by three passages through a chilled French pressure cell (Aminco, Silver Spring, Md.) at 27.5 MPa. After centrifugation at 17,400 × *g* for 1 h, the supernatant was used for enzyme activity measurements.

Protein determination, SDS-PAGE, and Western blot analysis. Protein concentrations were determined by the modified Lowry method of Hess et al. (19). Proteins were resolved by SDS-PAGE (28). Western blot analysis with antibodies raised to purified ISPα was performed as described by Zamanian and Mason (55). To determine the ISPα concentration expressed per milligram of cell extract protein, samples were resolved by SDS-PAGE, stained with Coomassie brilliant blue R250, and subjected to quantitative image analysis with the EASY-Win program (Herolab, Wiesloch, Germany). Duplicate samples (5 and 10 μg of cell extract protein) were taken, and a calibration curve was constructed by using a range of concentrations of pure $ISP_{BED}\alpha$ (1 to 15 μg).

Oxygen uptake measurement. Dioxygenase activities of cell extracts were determined polarographically by measuring O_2 consumption with a Clark-type oxygen electrode as previously described (11). The assay mixture contained 0.42 mM NADH, 0.5% (vol/vol) Triton X-100, 0.1 mM ferrous ammonium sulfate, and 1.5 mg of cell extract protein from the strain expressing $reductase_{BED}$ and $ferredoxin_{BED}$ (plasmid pJRM503). The following enzymes were also added to the assay mixture: for the coexpressed enzymes, 1.5 mg of cell extract protein from the strains expressing $ISP_{BED}\alpha$-$ISP_{BED}\beta$ (plasmid pJRM502), $ISP_{TOD}\alpha$-$ISP_{BED}\beta$ (plasmid pJRM502-1), or $ISP_{BOD}\alpha$-$ISP_{BED}\beta$ (plasmid pJRM502-2); and when the α and β subunits were expressed separately, 0.25 mg of ISP α subunits present in the cell extracts from the different strains and 0.5 mg of either

TABLE 2. Oligonucleotides used in this study

Oligonucleotide[a]	Oligonucleotide sequence[b]	Presence, loss, or gain of restriction site
Oligonucleotides for modification of the Shine-Dalgarno region		
KPIf[c]	5′ CTCGGTAC(CCAAAAAGT)GAGAAGACAATG 3′	Gain of KpnI
BEIIr[c]	5′ CAAGTAGCTGGTGACCTTCGGCCC 3′	BstEII
Mutant oligonucleotides[d]		
L285W	5′ CCAGCTACT**G**GACCGAAGGCCC**G**GCG 3′	Loss of DraII
A291S	5′ GAAGGCCCCGCGT**C**GGAAAAGGCGG 3′	Loss of SacII
G404D	5′ GCTGAGATG**TCC**ATGG**AC**CAAACCGTTG 3′	Gain of NcoI
I301V/T305S/I307L/L309V	5′ GCTC**GA**C**C**ATGA**GTTTGGA**GCCGCGCTC**CA**CACTAC 3′	Gain of BstXI
V324I/I327V	5′ CCCAGGT**A**TCAATAC**GGTCC**GAACATGG 3′	Gain of AvaII
I412V	5′ CGA**C**CC**GGTA**TACCCTGGTCG 3′	Gain of Bst1107I
K436R	5′ GCACATTGGC**TCCGGA**TGATGACC 3′	Gain of BspEI
E444D	5′ GACTGGGA**C**GCATTAAAGGCGACG 3′	Gain of BsmFI
Nonmutagenic oligonucleotides for PCR-based site-directed mutagenesis and/or cloning of *bod2C1*, *bod3C1*, *todC1-bedC2*, and *bodC1-bedC2* genes		
SBIf[c]	5′ CGTCAGACACTACGTACCTTCTCTGCC 3′	SnaBI
MUIr[c]	5′ TTAGGTTTAACGCGTCGCCTTTAATGC 3′	MluI
BEIIf[c]	5′ GGGCCGAAGGTCACCAGCTACTTG 3′	BstEII
SBIr[c]	5′ GGCAGAGAAGGTACGTAGTGTCTGACG 3′	SnaBI
HDIIIr[c]	5′ GGCTGAAAATCTTCTCTCATCCGC 3′	HindIII
PKK[c]	5′ GCGGATAACAATTTCACACAGG 3′	EcoRI
AGIr	5′ CGGGCGCTACCGGTGCCGGC 3′	AgeI[e]

[a] Most oligonucleotides were synthesized by Phil Marsh (King's College London); the exceptions were KPIf and BEIIr, which were synthesized by Pharmacia (UK) and Perkin-Elmer Ltd., respectively.

[b] The base changes are indicated by boldface type. The underlined bases indicate loss or addition of the restriction site. Additional bases are in parentheses.

[c] For the locations of nonmutagenic oligonucleotides see the positions of restriction sites in Fig. 1, sequences are within or close to the primer sequence.

[d] In the mutant oligonucleotide designations the first letter is the amino acid in the $ISP_{BED}\alpha$ sequence, the number corresponds to the position in the amino acid sequence, and the second letter is the replacing amino acid in the $ISP_{TOD}\alpha$ sequence.

[e] The AgeI restriction site is located between the *bedC1* and *bedC2* genes in the pJRM502 plasmid.

$ISP_{BED}\beta$ present in the cell extract from the strain containing plasmid pJRM505 or $ISP_{TOD}\beta$ present in the cell extract from the strain containing plasmid pJRM711. The reaction was initiated by addition of 300 μM benzene, toluene, or ethylbenzene dissolved in buffer. Enzyme activity was expressed in nanomoles of O_2 per minute per milligram of ISPα.

Enzyme activity. Benzene dioxygenase activity was determined by using ^{14}C-labeled substrates by measuring the accumulation of nonvolatile products on TLC squares by using a modification of the method described by Jiang et al. (22). Each reaction mixture (0.5 ml) was similar to the reaction mixture described for the polarographic assay, except that after 5 min of preincubation at room temperature, 1 mM NADH and either 20 μl of L-[U-^{14}C]benzene, 20 μl of L-[U-^{14}C]toluene (Sigma) in methanol (22.2×10^4 dpm μl^{-1}; final concentration, 0.8 mM), or 20 μl of L-[U-^{14}C]ethylbenzene (Sigma) in methanol (4.8×10^4 dpm μl^{-1}; final concentration, 0.8 mM) were added. The enzyme specific activity was expressed in nanomoles of total product formed per minute per milligram of ISPα.

Detection and quantification of reaction products. The oxidation products of the recombinant proteins from the different substrates were determined by using a modified method described by Ensley et al. (7). The assay with a radiolabeled substrate was allowed to proceed for 45 min. Aliquots (8 μl for experiments in which [^{14}C]benzene and [^{14}C]toluene were used and 16 μl for experiments in which [^{14}C]ethylbenzene was used) were applied to the origin of a TLC plate (Silica Gel 60 F254; thickness, 0.2 mm). Standard samples of *cis*-3,5-cyclohexadiene-1,2-diol, catechol, 3-methylcatechol, *o*-cresol, *m*-cresol, *p*-cresol, and benzyl alcohol were also applied to the chromatograms, which were air dried for 30 min and developed with chloroform-acetone (80:20, vol/vol). Radioactive spots were located by autoradiography with X-ray film exposed at −70°C for 6 days before development. The area containing the radioactive product was scraped from the TLC plate, and the amount of each nonvolatile ^{14}C-labeled product was determined by scintillation counting. Nonradioactive compounds were detected by spraying the plate with 2% (wt/vol) 2,6-dichloroquinone-4-chloroimide (13).

The identities of the reaction products were further established by GC-MS. Assays with unlabeled substrates were performed as described above, and the reaction products were extracted with 2 volumes of ethyl acetate. The organic phase was dried over anhydrous sodium sulfate, and the samples were concentrated to 100 μl under a flow of nitrogen. Samples were injected into a Hewlett-Packard 6890 GC coupled to a 5970 mass selective detector operating in splitless mode (injector temperature, 300°C) with a fused silica capillary column (inside diameter, 0.25 mm; length, 25 m) coated with a 0.1-μm phase of DB-5 (5% phenyl, 95% dimethylpolysiloxane; J& W Scientific, Folsom, Calif.). The column was kept at 50°C for 3 min, and then the temperature was increased to 300°C at a rate of 15°C/min and finally kept at 300°C for 10 min. The detector was operated in the scan mode with electron impact ionization at 70 eV and with scanning from 550 to 50 atomic mass units with a scan time of 0.86 s. The transfer line temperature was 280°C. All products were identified either by comparison of their GC-MS properties (retention times and mass fragments) with those of reference compounds used in the TLC experiments or by interpretation of the mass spectra. Relative yields of products were determined by integration of total ion current peak areas.

RESULTS

Chimeric proteins were constructed with the sequences containing residues 1 to 280 and 281 to 450 of $ISP_{BED}\alpha$ and $ISP_{TOD}\alpha$, which yielded proteins designated $ISP_{BOD}\alpha$ and $ISP_{TED}\alpha$ (Fig. 1A). Two additional chimeric α subunits in the C-terminal region were constructed. $ISP_{BOD2}\alpha$ contained the N-terminal region of $ISP_{BED}\alpha$ (residues 1 to 363) linked to the C-terminal region of $ISP_{TOD}\alpha$ (residues 364 to 450). $ISP_{BOD3}\alpha$ was $ISP_{BED}\alpha$ with residues 281 to 363 replaced with the residues of $ISP_{TOD}\alpha$. The cell extracts from each of the recombinant strains contained a protein that immunocross-reacted with a band whose relative mobility was identical to that of

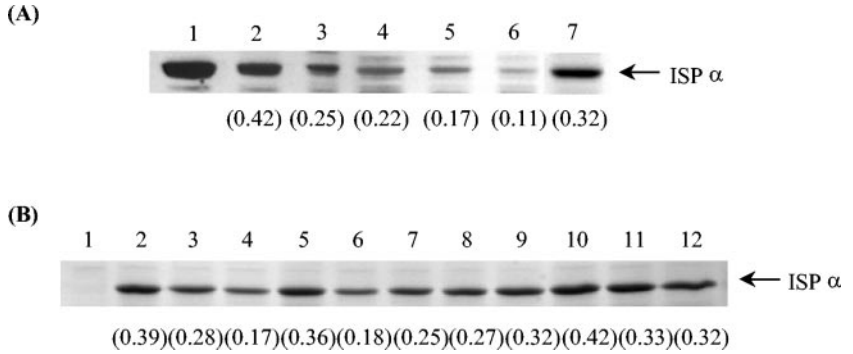

FIG. 2. SDS-PAGE-resolved *E. coli* cell extracts expressing recombinant ISP α subunits. The numbers in parentheses indicate the levels of expression of the soluble ISP α subunit in the cell extract (in milligrams per milligram of total protein; means of two determinations). (A) Wild-type and chimeric ISP α-subunit cell extracts. Lane 1, purified $ISP_{BED}\alpha$ (2 μg); lanes 2 to 7, cell extracts (5 μg of protein per lane) from *E. coli* strains containing plasmids pJRM504 ($ISP_{BED}\alpha$), pJRM5041 ($ISP_{BOD}\alpha$), pJRM5042 ($ISP_{TOD}\alpha$), pJRM5043 ($ISP_{TED}\alpha$), pJRM5041-2 ($ISP_{BOD3}\alpha$), and pJRM5041-1 ($ISP_{BOD2}\alpha$), respectively. (B) Wild-type and mutant ISP α subunit cell extracts. Lanes 1 to 12, cell extracts (5 μg of protein per lane) from *E. coli* strains containing plasmids pKK223-3, pJRM504 ($ISP_{BED}\alpha$), pJRM504M1 [$ISP_{BED}\alpha$(L285W)], pJRM504M2 [$ISP_{BED}\alpha$(A291S)], pJRM504M7 [$ISP_{BED}\alpha$(G404D)], pJRM504M3 [$ISP_{BED}\alpha$(L285W/A291S)], pJRM504M6 [$ISP_{BED}\alpha$(L285W/A291S/G404D)], pJRM504M4 [$ISP_{BED}\alpha$(I301V/T305S/I307L/L309V)], pJRM504M5 [$ISP_{BED}\alpha$(V324I/I327V)], pJRM504M8 [$ISP_{BED}\alpha$(I412V)], pJRM504M9 [$ISP_{BED}\alpha$(K436R)], and pJRM504M10 [$ISP_{BED}\alpha$(E444D)], respectively.

purified $ISP_{BED}\alpha$ (data not shown). The level of protein production was determined by quantitative SDS-PAGE (Fig. 2A). Despite the presence of identical promoter and ribosome-binding sites, the level of expression for the recombinant plasmids generally was not as high as that for the $ISP_{BED}\alpha$ protein (Fig. 2A, lane 2).

When the O_2 uptake assay was used to measure activity, all the recombinant ISP α subunits reconstituted with $ISP_{BED}\beta$ or $ISP_{TOD}\beta$ were active with the three substrates (Fig. 1 and Table 3). The ratios of the oxygen uptake rates measured with toluene or ethylbenzene to the oxygen uptake rates measured with benzene (Fig. 1) gave a first measure of the substrate preferences of the enzymes. The chimeric $ISP_{BOD}\alpha$ and $ISP_{BOD3}\alpha$ proteins combined with $ISP_{BED}\beta$ had a pattern of substrate specificity more like that of $ISP_{TOD}\alpha$; the toluene/benzene activity ratios of the three proteins were 1.07, 0.88, and 1.26, respectively, and the ethylbenzene/benzene activity ratios were 1.10, 0.94, and 1.20, respectively. Furthermore, $ISP_{TED}\alpha$ and $ISP_{BOD2}\alpha$ were more similar to $ISP_{BED}\alpha$, and the ethylbenzene/benzene activity ratios of the three proteins were 0.35, 0.30, and 0.21, respectively (Fig. 1). The nature of the β subunit did not have a consistent effect on the substrate specificity. It should be noted that the specific activities of $ISP_{TOD}\alpha$, $ISP_{BOD}\alpha$, $ISP_{TED}\alpha$, and $ISP_{BOD3}\alpha$ combined with $ISP_{BED}\beta$ were lower than the specific activity of $ISP_{BED}\alpha$ (Table 3). However, this had no effect on the substrate preference since it was the relative activity with all three substrates that was important.

The results for the chimeric α subunits (Fig. 1A) revealed that a region of the protein responsible for specificity was between residues 281 and 450. In this region, benzene and

TABLE 3. Comparison of the rates of oxygen uptake and nonvolatile product formation by different ISP α subunits combined with ISP_{BED} β subunit[a]

Source of ISP α subunit in assay (plasmid)	Type of assay	Sp act (nmol of O_2 min^{-1} mg^{-1} or nmol of product min^{-1} mg^{-1})			% of uncoupling		
		Benzene	Toluene	Ethylbenzene	Benzene	Toluene	Ethylbenzene
ISP_{BED} (pJRM504)	Polarographic	115 ± 9.6[b]	70.5 ± 5.5	25 ± 1.5	0	22	0
	Radiolabeled	120 ± 2.9	54.9 ± 1.9	30.7 ± 1.7			
ISP_{TOD} (pJRM5042)	Polarographic	44.9 ± 2.2	56.4 ± 3.9	54.1 ± 3.4	0	0	21
	Radiolabeled	45.5 ± 0.7	61.3 ± 2.5	42.5 ± 3.4			
ISP_{BOD} (pJRM5041)	Polarographic	44.5 ± 3.1	47.5 ± 4.1	49.1 ± 5.6	0	0	45
	Radiolabeled	47.6 ± 2.6	46.2 ± 0.7	26.8 ± 2.3			
ISP_{TED} (pJRM5043)	Polarographic	39.1 ± 2.3	25.3 ± 3.0	13.8 ± 0.5	0	0	48
	Radiolabeled	42.1 ± 2.9	25.5 ± 1.7	8.8 ± 0.7			
ISP_{BOD2} (pJRM5041-1)	Polarographic	112 ± 8.5	79.7 ± 8.1	33.7 ± 4.1	0	37	24
	Radiolabeled	115 ± 2.9	49.6 ± 2.2	25.7 ± 2.6			
ISP_{BOD3} (pJRM5041-2)	Polarographic	36.8 ± 4.6	32.2 ± 6.1	34.5 ± 4.0	0	0	31
	Radiolabeled	39.1 ± 1.5	32.2 ± 0.6	23.6 ± 2.5			
I301V/T305S/I307L/L309V (pJRM504M4)	Polarographic	84.5 ± 4.4	62.1 ± 8.9	70.7 ± 9.9	0	0	44
	Radiolabeled	85.1 ± 1.9	70.8 ± 6.1	39.9 ± 1.4			

[a] Activities were determined with ISP_{BED} β subunit, $ferredoxin_{BED}$, and $reductase_{BED}$ cell extracts. The specific activity is expressed as the rate of O_2 uptake measured polarographically (three determinations) or as the amount of nonvolatile ^{14}C-labeled product formed from oxidation of [^{14}C]benzene, [^{14}C]toluene, and [^{14}C]ethylbenzene (nine determinations).

[b] Mean ± standard deviation.

toluene dioxygenases differ at 12 amino acid positions. Single and multiple amino acid mutations were generated, in which the nonconserved residues of $ISP_{BED}\alpha$ were replaced by the corresponding residues of $ISP_{TOD}\alpha$ (Fig. 1B). The ISPα concentration was estimated by quantitative SDS-PAGE (Fig. 2B) to be between 0.17 and 0.42 mg mg of protein^{-1}. When the activity was measured polarographically, the majority of the mutant proteins had a substrate preference similar to that of the wild type. However, $ISP_{BED}\alpha$(I301V/T305S/I307V/L309V) showed an increased preference for ethylbenzene, with an ethylbenzene/benzene activity ratio of 0.84 (Fig. 1B).

Table 3 shows the rates of product formation measured by ^{14}C assays for a representative range of recombinant proteins combined with $ISP_{BED}\beta$, and the data were compared with the rates of oxygen uptake under the same conditions, as shown in Fig. 1. The difference between the rate of product formation and the rate of oxygen consumption represented the rate of uncoupled oxidation of NADH. With benzene as the substrate, the rate of O_2 consumption for $ISP_{BED}\alpha$ was equal to the amount of products formed, which was indicative of tight coupling, but for the chimeric proteins uncoupling was observed with toluene and, more particularly, with ethylbenzene. For example, the percentage of uncoupling (percentage of O_2 consumed in excess of the amount of product formed) was 45% for $ISP_{BOD}\alpha$ and 44% for $ISP_{BED}\alpha$(I301V/T305S/I307L/L309V), both with ethylbenzene (Table 3). Similar uncoupling reactions have been observed with naphthalene dioxygenase, in which the oxidation of benzene, toluene, and ethylbenzene was partially uncoupled from O_2 consumption (29, 31). However, the ethylbenzene/benzene activity ratios as determined by the radiolabel assay were 0.67 for $ISP_{BOD}\alpha$ and 0.71 for $ISP_{BOD3}\alpha$, compared to 0.23 for $ISP_{BED}\alpha$ (Table 3), indicating that these enzymes had a higher substrate preference for ethylbenzene than the wild type. This phenomenon was less pronounced for $ISP_{BED}\alpha$(I301V/T305S/I307L/L309V) which had a ratio of 0.47.

The products formed from the three substrates were investigated. Samples from ^{14}C assays of the recombinant proteins, either expressed separately or coexpressed ($ISP_{BED}\alpha$-$ISP_{BED}\beta$, $ISP_{TOD}\alpha$-$ISP_{BED}\beta$, and $ISP_{BOD}\alpha$-$ISP_{BED}\beta$), were subjected to TLC (Fig. 3). With benzene as the substrate, a single compound with an R_f of 0.25, corresponding to the reference compound benzene *cis*-dihydrodiol, was detected in every case (Fig. 3A). This result is consistent with previous studies (12). With toluene as the substrate, two compounds (R_f, 0.31 and 0.67) were detected (Fig. 3B). By analogy to the benzene dioxygenase product, the compound with an R_f of 0.31 was provisionally identified as the expected *cis*-2,3-dihydroxy-1-methyl-cyclohexa-4,6-diene (toluene *cis*-dihydrodiol) (12). The R_f of 0.67 corresponded to the R_f of benzyl alcohol. Similarly, with all the dioxygenases that oxidized ethylbenzene, two compounds with R_f values of 0.35 and 0.71 were detected (Fig. 3C), and these compounds were provisionally identified as *cis*-2,3-dihydroxy-1-ethyl-cyclohexa-4,6-diene (ethylbenzene *cis*-dihydrodiol) and 1-phenethyl alcohol, respectively.

The products of the reactions described above, but without the use of radiolabeled substrates, were further analyzed by GC-MS (Tables 4 and 5). Since some compounds are known to undergo thermal decomposition during analysis, the phenol and catechols that were detected by GC-MC and not by other methods were interpreted as being the products of thermal dehydration of the *cis*-diols. Thus, with benzene as the substrate, peaks with masses corresponding to those of phenol, benzene *cis*-dihydrodiol, and catechol were detected, and the sum of the masses of these peaks corresponded to the mass of the single product, presumed to be benzene *cis*-dihydrodiol, observed in the autoradiogram (Fig. 3A).

When toluene was used, toluene *cis*-dihydrodiol and *o*- and *m*-cresols, the expected dehydration products, were detected (Table 5); again, the sum of the levels of these products was taken to represent the level of *cis*-diols produced. In addition, benzyl alcohol and benzaldehyde were observed only in trace amounts with ISP_{TOD}, but the amounts were larger with ISP_{BED}. In principle, the benzyl alcohol could be formed either by direct monohydroxylation of toluene by benzene dioxygenase or by production of toluene *cis*-dihydrodiol, followed by dehydration and isomerization to benzyl alcohol. This possibility was eliminated by mixing $ISP_{TOD}\alpha$ and $ISP_{BED}\beta$ in a dioxygenase assay mixture and allowing them to react with [^{14}C]toluene to produce the *cis*-dihydrodiol. The preparation was then further incubated with a reaction mixture containing $ISP_{BED}\alpha$ and $ISP_{BED}\beta$, and the results were analyzed by TLC. No further formation of benzyl alcohol was observed (data not shown). Therefore, the benzyl alcohol was the result of chain monohydroxylation of the substrate by the enzyme system; benzaldehyde was most probably the direct product of further oxidation of benzyl alcohol by the dioxygenase. Analogous reactions have been observed during oxidation of toluene by naphthalene dioxygenase (30) and xylene monooxygenase (18). However, the possibility that a nonspecific host alcohol dehydrogenase caused the conversion of benzyl alcohol to benzaldehyde cannot be ruled out.

Similarly, for ethylbenzene, in addition to the *cis*-dihydrodiol detected in the autoradiogram analysis, the dehydration products 2- and 3-hydroxyethylbenzene were observed by GC-MS (Table 5). As observed for the oxidation of toluene, ethylbenzene was monohydroxylated on its side chain to form 1-phenethyl alcohol. Lee and Gibson (31) reported that naphthalene dioxygenase oxidized ethylbenzene to 1-phenethyl alcohol, followed by slower oxidation of the latter compound to acetophenone. This rate-determining step (31) may explain why acetophenone was not observed.

Table 5 shows that all of the enzymes tested catalyzed the side chain monohydroxylation of toluene and ethylbenzene. The products were quantified by TLC (Fig. 3), and in general, toluene dioxygenase was more efficient than benzene dioxygenase in the dihydroxylation of toluene and produced less of the monohydroxylation products benzyl alcohol and benzaldehyde. $ISP_{BED}\alpha$(I301V/T305S/I307L/L309V) was intermediate between these two proteins. As expected for benzene, which has no side chains to be oxidized, no products other than the dihydrodiol were detected.

DISCUSSION

In this work, sections and individual amino acids of the toluene dioxygenase sequence were replaced in the benzene dioxygenase α subunit in order to probe the regions responsible for substrate preference for toluene and ethylbenzene. All of the ISP α subunits were active when they were combined

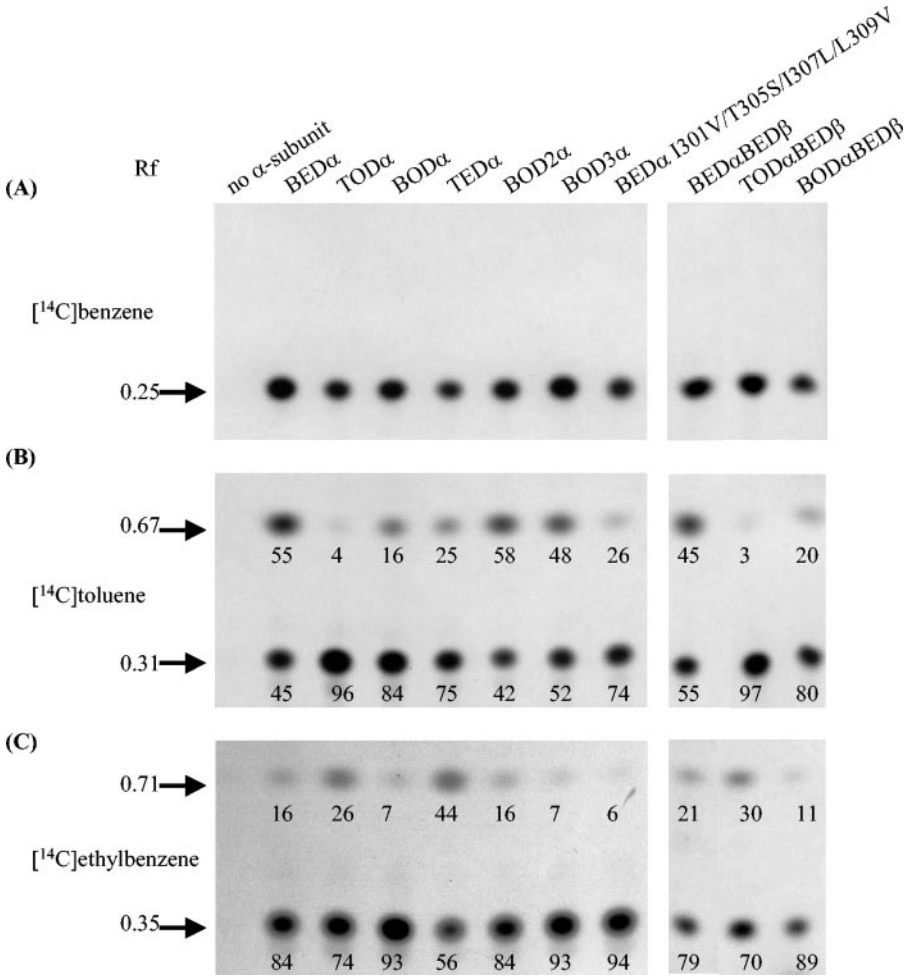

FIG. 3. Autoradiograms of the products formed by using [^{14}C]benzene (A), [^{14}C]toluene (B), and [^{14}C]ethylbenzene (C) by wild-type, chimeric, and mutant $ISP_{BED}\alpha$ subunits combined with the $ISP_{BED}\beta$ subunit and coexpressed $ISP_{BED}\alpha$-$ISP_{BED}\beta$, $ISP_{TOD}\alpha$-$ISP_{BED}\beta$, and $ISP_{BOD}\alpha$-$ISP_{BED}\beta$ in the dioxygenase assay. The R_f values of the radiolabeled products are indicated on the left. The numbers on the autoradiograms indicate the percentages of the chain monohydroxylated and *cis*-diol products. The values are averages of two determinations. A repeat experiment gave similar results. Details of the experiment are described in Materials and Methods.

with β subunits in vitro, in contrast to some other dioxygenases, in which the α and β subunits must be coexpressed to form a functional enzyme (10, 20, 46, 48). The $ISP_{BOD3}\alpha$ chimera narrows the region for substrate preference for alkylbenzenes between residues 281 and 363. In this region, the amino acid substitutions I301V, T305S, I307L, and L309V resulted in a recombinant enzyme with a rate of O_2 uptake with ethylbenzene that was substantially higher than that of the wild type (Table 3). The dioxygen data combined with the amount of nonvolatile products showed that for some of the ISP α subunits tested, partial uncoupling of O_2 consumption was observed with toluene and, more particularly, with ethylbenzene. The first product of uncoupled reduction of O_2 is expected to be H_2O_2 from the protonation of iron-bound peroxide species, as proposed for cytochrome P450 (14). However, formation of H_2O_2 is not observed as a result of uncoupling in assays of benzene dioxygenase (1). As suggested by Lee (29), this could be due to iron-catalyzed Fenton chemistry with H_2O_2 and, ultimately, water as the final product. $ISP_{BOD}\alpha$ and $ISP_{BOD3}\alpha$ in which partial uncoupling reactions were observed did have higher substrate specificity for ethylbenzene than the wild-type $ISP_{BED}\alpha$. However, the amino acids I301, T305, I307, and L309 are not the only amino acids involved in substrate specificity because although they increased the substrate preference for ethylbenzene, the high uncoupling reaction (44% with ethylbenzene) made them less efficient than the wild-type ISP_{TOD}.

There was no discernible correlation between the degree of uncoupling and the type of ISP α subunit in the assay; for example, $ISP_{BED}\alpha$ showed partial uncoupling of oxygen consumption with toluene (22%), while $ISP_{TED}\alpha$, which contained the same C-terminal region, showed no significant uncoupling with the same substrate. However, ethylbenzene, which had the largest substituent, induced uncoupling of O_2 uptake in most cases, indicating that substrate shape or size is a factor. The fact that the specific activities of some of the chimeric α subunits combined with $ISP_{BED}\beta$ were lower with all three substrates (Table 3) than the specific activity of wild-type $ISP_{BED}\alpha$ could be explained by some mismatch at the subunit interface in the heterologous α-β pair, although, as indicated

TABLE 4. Gas chromatography-mass spectrometric results for reaction products

Ion[a]	Retention time (min)	Product [ion mass (relative abundance)]
Phenol	5.0	94 (100), 66 (38), 65 (28), 63 (9), 55 (9), 51 (7)
Benzene *cis*-dihydrodiol	5.3	12 (15), 94 (23), 83 (36), 68 (26), 66 (100), 65 (32), 55 (40)
Catechol	7.8	110 (100), 92 (12), 81 (19), 64 (47), 63 (23), 53 (18)
Benzaldehyde	4.5	106 (82), 105 (82), 77 (100), 51 (53)
Benzyl alcohol	5.7	108 (73), 107 (49), 79 (100), 77 (59), 51 (31)
o-Cresol	6.0	108 (100), 107 (90), 90 (25), 79 (54), 77 (51), 51 (25)
m-Cresol	6.3	108 (100), 107 (94), 79 (47), 77 (46), 53 (16), 51 (19)
Toluene *cis*-dihydrodiol	6.4	126 (7), 108 (60), 97 (21), 80 (82), 79 (100), 77 (36), 65 (23), 55 (22) 53 (22) 51 (20)
Phenethyl alcohol	6.0	122 (20), 107 (77), 79 (100), 77 (57), 51 (29)
2-Hydroxyethylbenzene	7.0	122 (39), 107 (100), 79 (17), 77 (34), 51 (10)
3-Hydroxyethylbenzene	7.4	122 (41), 107 (100), 79 (10), 77 (32), 51 (8)
Ethylbenzene *cis*-dihydrodiol	7.5	140 (8), 122 (8), 111 (19), 94 (40), 84 (49), 83 (86), 81 (30), 79 (38), 68 (49), 67 (31), 57 (46), 55 (100), 53 (28), 51 (17)

[a] All the products formed by dioxygenase-catalyzed reactions with $ISP_{BED}\alpha$, $ISP_{TOD}\alpha$, or $ISP_{BED}\alpha$(I301V/T305S/I307L/L309V) combined with the ISP_{BED} β subunit by using benzene, toluene, or ethylbenzene as the substrate.

above, this would not have any effect on the relative activity with the substrates. The source of the β subunit had no systematic effect on substrate specificity (Fig. 1).

Analysis of product formation indicated that both dihydroxylation and chain monohydroxylation occurred in all the recombinant ISP α subunits combined with ISP β subunits. Several studies have reported that dioxygenases, such as toluene dioxygenase (4, 32, 40–42, 51), catalyze monohydroxylation reactions. However, to our knowledge, this study is the first study to report the chain monohydroxylation of toluene and ethylbenzene by benzene dioxygenase to form benzyl alcohol and 1-phenethyl alcohol, respectively. The amounts of *cis*-diols and chain monohydroxylated products were similar whether the ISP α and β subunits were expressed separately or not (Fig. 3), confirming that the two subunits can combine with each other to form a functional enzyme. For example, around 50% of toluene *cis*-dihydrodiol and benzyl alcohol was produced with $ISP_{BED}\alpha$ and coexpressed $ISP_{BED}\alpha$-$ISP_{BED}\beta$ when toluene was the substrate. This also showed that the amount of *cis*-diols and chain monohydroxylated compounds depended upon the nature of the α subunit in the assay. Furthermore, $ISP_{TOD}\alpha$, $ISP_{BOD}\alpha$, and $ISP_{BOD3}\alpha$, all of which had the C-terminal region of ISP_{TOD}, had different amounts of chain monohydroxylated products (for example, 4, 16, and 48% benzyl alcohol, respectively), indicating that no region of the ISP α subunit seemed to correlate with the amount of the benzyl and 1-phenethyl alcohols.

We modeled the sequence of the $ISP_{BED}\alpha$(I301V/T305S/I307L/L309V) by homology with the known structure of naphthalene dioxygenase (25) (Fig. 4). As determined by sequence comparisons, I301V, T305S, I307L, and L309V correspond to V287, I291, R293, and H295 in naphthalene dioxygenase. Surprisingly, these residues are not in the active site cavity, nor do they line the channel leading from this site to the surface. H295 is located behind F352, and modification of the latter amino acid has been shown to alter the regiospecificity of naphthalene dioxygenase (39). L307 in toluene dioxygenase corresponds to the residue which was shown by Zhang et al. (56) (by using substitution in a proline) to change the proportion of 1-indenol, 1-indanone, and *cis*-indandiol produced. The other amino acids are aligned adjacent to residues lining the substrate channel. Replacement of I301 and L309 in benzene dioxygenase by

TABLE 5. Percentages of products formed by dioxygenase-catalyzed reactions with $ISP_{BED}\alpha$, $ISP_{TOD}\alpha$, or $ISP_{BED}\alpha$(I301V/T305S/I307L/L309V) combined with the ISP_{BED} β subunit by using benzene, toluene, or ethylbenzene as the substrate

Substrate	Product	% of product formed[a]		
		$ISP_{BED\alpha}$	$ISP_{TOD\alpha}$	$ISP_{BED\alpha}$ mutant
Benzene	Benzene *cis*-dihydrodiol	46	37	42
	Phenol[b]	35	30	37
	Catechol[b]	19	33	21
Toluene	Toluene *cis*-dihydrodiol	3	45	12
	Benzaldehyde	18	1	8
	Benzyl alcohol	53	6	31
	o-Cresol[b]	22	38	42
	m-Cresol[b]	4	10	7
Ethylbenzene	Ethylbenzene *cis*-dihydrodiol	5	24	16
	1-Phenethyl alcohol	24	39	5
	2-Hydroxyethylbenzene[b]	58	30	65
	3-Hydroxyethylbenzene[b]	13	7	14

[a] The values are averages of two determinations. A repeat experiment gave similar results.
[b] Product expected from thermal decomposition. See text for details.

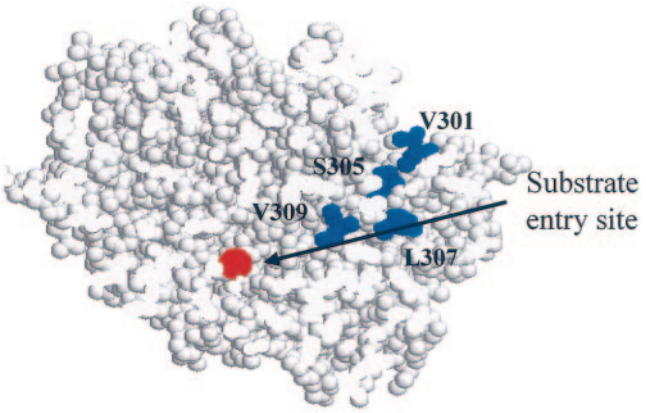

FIG. 4. Structural representation of the putative substrate entry channel in $ISP_{BED}\alpha$(I301V/T305S/I307L/L309V). The protein is represented in spacefill. Iron is indicated by red, and the four amino acid substitutions (I301V, T305S, I307L, and L309V) are indicated by blue spheres. The view is a section through the substrate channel, and the arrow indicates the putative route that the substrate takes to get to the iron catalytic site. The model was generated with the SWISS-MODEL program (15; http://expasy.hcuge.ch/swissmod/SWISS-MODEL.html) and was displayed by using RasWin Molecular Graphics Window, version 2.6 (43).

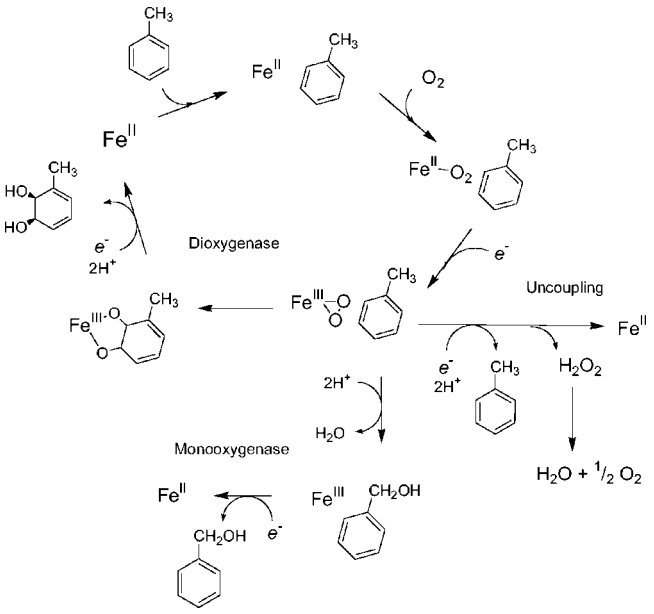

FIG. 5. Alternative pathways for dioxygenase and monooxygenase activities and uncoupling. Dihydroxylation results from the addition of O_2 and two-electron reduction to the peroxo derivative. In the structure of naphthalene dioxygenase with O_2 and substrate in the active site (24), the oxygen is bound side-on to the iron and next to the aromatic ring. Addition of both oxygen atoms, with two protons, would lead to addition of two —OH groups. The monooxygenation reactions are concerted reactions in which one oxygen atom is protonated and reduced to H_2O and the other oxygen atom is inserted into the C—H bond of the side chain. The uncoupling reaction is shown as a protonation of the Fe-peroxo species, releasing H_2O_2.

the less bulky amino acid valine should facilitate access to the larger substrates, such as toluene and ethylbenzene, either by decreasing steric hindrance or by increasing flexibility in the channel lining. Although the amino acids surrounding the binding site for the aromatic ring are unchanged, the effects of the mutations on the conformational flexibility of the substrate cavity are difficult to predict. The consequences of the combination are a higher rate of oxygen uptake for toluene and ethylbenzene but a high rate of uncoupling, especially with ethylbenzene. Some monohydroxylated products were observed, but the amount was intermediate between the amounts for all the novel enzymes. The uncoupling is not directly associated with the formation of the chain monohydroxylated product because $ISP_{BED}\alpha$(I301V/T305S/I307L/L309V) had a high level of uncoupling with ethylbenzene yet produced the largest proportion of *cis*-diols.

One must assume that the native enzymes evolved to maximize the dihydroxylation of the preferred substrates to the required stereospecific products and to avoid the side reactions. From the crystal structures of naphthalene dioxygenase it is clear that the position of the substrate relative to the Fe-bound O_2 is favorable for the dioxygenase reaction (24). The three different reactions, dihydroxylation, monohydroxylation, and uncoupled reduction of O_2 to H_2O_2, may be considered to be the result of competing pathways in the oxidoreduction reactions of iron with oxygen (Fig. 5). Wolfe et al. (52, 53) have shown that there is strict control of the redox events within the enzyme. To avoid uncontrolled reduction of O_2, electron transfer from the Rieske cluster to Fe(III) does not occur until substrate is present in the active site, and the product is not released until the iron is reduced to Fe(II) for the next cycle. The dihydroxylation of the substrate by the adjacent side-on peroxo complex is the dominant reaction for native benzene and toluene dioxygenases. However, in the chimeric enzymes the shape of the substrate channel is distorted, and it is possible that the substrate is less tightly bound than it is in the native enzyme. Movement of the substrate away from the binding pocket should allow the side chain hydroxylation, possibly by repositioning of the substrate in the active site, and the uncoupling reaction with reduction to water. Thus, the different product ratios can be understood in terms of the tightness of binding of the substrate to the active site. Following the course of directed evolution seems to be a promising strategy for the engineering of enzymes to metabolize novel substrates.

ACKNOWLEDGMENTS

This work was supported by a grant from the United Kingdom Natural Environment Research Council (grant GR3/R9674) and by a TMR Network grant from the European Commission (grant CERB FMRX CT 980174, NOHEMIP).

We thank S. Anguravirutt and C. Butler for providing recombinant strains and S. Jickells for assistance with the GC-MS experiments.

REFERENCES

1. **Axcell, B. C., and P. J. Geary.** 1975. Purification and some properties of a soluble benzene-oxidizing system from a strain of *Pseudomonas*. Biochem. J. **146:**173–183.
2. **Barriault, D., M. M. Plante, and M. Sylvestre.** 2002. Family shuffling of a targeted *bphA* region to engineer biphenyl dioxygenase. J. Bacteriol. **184:** 3794–3800.
3. **Barriault, D., C. Simard, H. Chatel, and M. Sylvestre.** 2001. Characterisation of hybrid biphenyl dioxygenases obtained by combining *Burkholderia* sp. strain LB400 *bphA* with the homologous gene of *Comamonas testosteroni* B-356. Can. J. Microbiol. **47:**1025–1032.
4. **Brand, J. M., D. L. Cruden, G. J. Zylstra, and D. T. Gibson.** 1992. Stereospecific hydroxylation of indan by *Escherichia coli* containing the cloned toluene

dioxygenase genes from *Pseudomonas putida* F1. Appl. Environ. Microbiol. **58:**3407–3409.
5. **Bruhlmann, F., and W. Chen.** 1999. Tuning biphenyl dioxygenase for extended substrate specificity. Biotechnol. Bioeng. **63:**544–551.
6. **Butler, C. S., and J. R. Mason.** 1997. Structure-function analysis of the bacterial aromatic ring-hydroxylating dioxygenases. Adv. Microb. Physiol. **38:**47–84.
7. **Ensley, B. D., D. T. Gibson, and A. L. Laborde.** 1982. Oxidation of naphthalene by a multicomponent enzyme system from *Pseudomonas* sp. strain NCIB 9816. J. Bacteriol. **149:**948–954.
8. **Erickson, B. D., and F. J. Mondello.** 1993. Enhanced biodegradation of polychlorinated biphenyls after site-directed mutagenesis of a biphenyl dioxygenase gene. Appl. Environ. Microbiol. **59:**3858–3862.
9. **Furukawa, K., J. Hirose, S. Hayashida, and K. Nakamura.** 1994. Efficient degradation of trichloroethylene by a hybrid aromatic ring dioxygenase. J. Bacteriol. **176:**2121–2123.
10. **Furukawa, K., J. Hirose, A. Suyama, T. Zaiki, and S. Hayashida.** 1993. Gene components responsible for discrete substrate-specificity in the metabolism of biphenyl (Bph operon) and toluene (Tod operon). J. Bacteriol. **175:**5224–5232.
11. **Geary, P. J., J. R. Mason, and C. L. Joannou.** 1990. Benzene dioxygenase from *Pseudomonas putida* (NCIB 12190). Methods Enzymol. **188:**52–60.
12. **Gibson, D. T., G. E. Cardini, F. C. Maseles, and R. E. Kallio.** 1970. Incorporation of oxygen-18 into benzene by *Pseudomonas putida.* Biochemistry **9:**1631–1635.
13. **Gibson, D. T., M. Hensley, H. Yoshioka, and T. J. Mabry.** 1970. Formation of (+)-cis-2,3-dihydroxy-1-methylcyclohexa-4,6-diene from toluene by *Pseudomonas putida.* Biochemistry **9:**1626–1630.
14. **Guengerich, F. P.** 1991. Reactions and significance of cytochrome p-450 enzymes. J. Biol. Chem. **266:**10019–10022.
15. **Guex, N., and M. C. Peitsch.** 1997. SWISS-MODEL and the Swiss-Pdb Viewer: an environment for comparative protein modelling. Electrophoresis **18:**2714–2723.
16. **Hanahan, D.** 1983. Studies on transformation of *Escherichia coli* with plasmids. J. Mol. Biol. **166:**557–580.
17. **Harayama, S., M. Kok, and E. L. Neidle.** 1992. Functional and evolutionary relationships among diverse oxygenases. Annu. Rev. Microbiol. **46:**565–601.
18. **Harayama, S., R. A. Leppik, M. Rekik, N. Mermod, P. R. Lehrbach, W. Reineke, and K. N. Timmis.** 1989. Gene order of the TOL catabolic upper pathway operon and oxidation of both toluene and benzylalcohol by the XylA product. J. Bacteriol. **167:**455–461.
19. **Hess, H. H., M. B. Lees, and J. E. Derr.** 1978. A linear Lowry-Folin assay for both water-soluble and sodium dodecyl sulphate-solubilised proteins. Anal. Biochem. **85:**295–300.
20. **Hirose, J., A., S. Suyama, K. Hayashida, and K. Furukawa.** 1994. Construction of hybrid biphenyl (*bph*) and toluene (*tod*) genes for functional analysis of aromatic ring dioxygenases. Gene **138:**27–33.
21. **Hudlicky, T., M., J. Mandel, R. S. Rouden, B. B. Lee, T. Dudding, K. J. Yost, and J. S. Merola.** 1994. Microbial oxidation of aromatics in enantiocontrolled synthesis. Part 1. Expedient and general asymmetric synthesis of inositols and carbohydrates via an unusual oxidation of a polarized diene with potassium permanganate. J. Chem. Soc. Perkin Trans. **1:**1553–1567.
22. **Jiang, H. Y., R. E. Parales, N. A. Lynch, and D. T. Gibson.** 1996. Site-directed mutagenesis of conserved amino acids in the alpha subunit of toluene dioxygenase: potential mononuclear non-heme iron coordination sites. J. Bacteriol. **178:**3133–3139.
23. **Kammann, M., J. Laufs, J. Schell, and B. Gronenborn.** 1989. Rapid insertional mutagenesis of DNA by polymerase chain reaction (PCR). Nucleic Acids Res. **17:**5404.
24. **Karlsson, A., J. V. Parales, R. E. Parales, D. T. Gibson, H. Eklund, and S. Ramaswamy.** 2003. Crystal structure of naphthalene dioxygenase: side-on binding of dioxygen to iron. Science **299:**1039–1042.
25. **Kauppi, B., K. Lee, E. Carredano, R. E. Parales, D. T. Gibson, H. Eklund, and S. Ramaswamy.** 1998. Structure of an aromatic-ring-hydroxylating dioxygenase-naphthalene 1,2-dioxygenase. Structure **6:**571–586.
26. **Kimura, N., A. Nishi, M. Goto, and K. Furukawa.** 1997. Functional analyses of a variety of chimeric dioxygenases constructed from two biphenyl dioxygenases that are similar structurally but different functionally. J. Bacteriol. **179:**3936–3943.
27. **Kunkel, T. A.** 1985. Rapid and efficient site-specific mutagenesis without phenotypic selection. Proc. Natl. Acad. Sci. USA **82:**488–492.
28. **Laemmli, U. K.** 1970. Cleavage of structural proteins during the assembly of the head of bacteriophage T4. Nature (London) **227:**680–685.
29. **Lee, K.** 1999. Benzene-induced uncoupling of naphthalene dioxygenase activity and enzyme inactivation by production of hydrogen peroxide. J. Bacteriol. **181:**2719–2725.
30. **Lee, K., and D. T. Gibson.** 1996. Stereospecific dihydroxylation of the styrene vinyl group by purified naphthalene dioxygenase from *Pseudomonas* sp. strain NCIB 9816–4. J. Bacteriol. **178:**3353–3356.
31. **Lee, K., and D. T. Gibson.** 1996. Toluene and ethylbenzene oxidation by purified naphthalene dioxygenase from *Pseudomonas* sp. strain NCIB 9816–4. Appl. Environ. Microbiol. **62:**3101–3106.
32. **Lehning, A., U. Fock, R. M. Wittich, K. N. Timmis, and D. H. Pieper.** 1997. Metabolism of chlorotoluenes by *Burkholderia* sp. strain PS12 and toluene dioxygenase of *Pseudomonas putida* F1: evidence for monooxygenation by toluene and chlorobenzene dioxygenases. Appl. Environ. Microbiol. **63:**1974–1979.
33. **Link, T. A., O. M. Hatzfeld, P. Unalkat, J. K. Shergill, R. Cammack, and J. R. Mason.** 1996. Comparison of the "Rieske" [2Fe-2S] center in the bc1 complex and in bacterial dioxygenases by circular dichroism spectroscopy and cyclic voltammetry. Biochemistry **35:**7546–7552.
34. **Maeda, T., Y. Takahashi, H. Suenaga, A. Suyama, M. Goto, and K. Furukawa.** 2001. Functional analyses of Bph-Tod hybrid dioxygenase, which exhibits high degradation activity toward trichloroethylene. J. Biol. Chem. **276:**29833–29838.
35. **Mason, J. R., C. S. Butler, R. Cammack, and J. K. Shergill.** 1997. Structural studies on the catalytic component of benzene dioxygenase from *Pseudomonas putida.* Biochem. Soc. Trans. **25:**90–95.
36. **Mondello, F. J., M. P. Turcich, J. H. Lobos, and B. D. Erickson.** 1997. Identification and modification of biphenyl dioxygenase sequences that determine the specificity of polychlorinated biphenyl degradation. Appl. Environ. Microbiol. **63:**3096–3103.
37. **Parales, J. V., R. E. Parales, S. M. Resnick, and D. T. Gibson.** 1998. Enzyme specificity of 2-nitrotoluene 2,3-dioxygenase from *Pseudomonas* sp. strain JS42 is determined by the C-terminal region of the alpha subunit of the oxygenase component. J. Bacteriol. **180:**1194–1199.
38. **Parales, R. E., M. D. Emig, N. A. Lynch, and D. T. Gibson.** 1998. Substrate specificities of hybrid naphthalene and 2,1-dinitrotoluene dioxygenase enzyme systems. J. Bacteriol. **180:**2337–2344.
39. **Parales, R. E., K. Lee, S. M. Resnick, H. Y. Jiang, D. J. Lessner, and D. T. Gibson.** 2000. Substrate specificity of naphthalene dioxygenase: effect of specific amino acids at the active site of the enzyme. J. Bacteriol. **182:**1641–1649.
40. **Phumathon, P., and G. M. Stephens.** 1999. Production of toluene cis-glycol using recombinant *Escherichia coli* strains in glucose-limited fed batch culture. Enzyme Microb. Technol. **25:**810–819.
41. **Robertson, J. B., J. C. Spain, J. D. Haddock, and D. T. Gibson.** 1992. Oxidation of nitrotoluenes by toluene dioxygenase: evidence for a monooxygenase reaction. Appl. Environ. Microbiol. **58:**2643–2648.
42. **Sakamoto, T., J. M. Joern, A. Arisawa, and F. H. Arnold.** 2001. Laboratory evolution of toluene dioxygenase to accept 4-picoline as a substrate. Appl. Environ. Microbiol. **67:**3882–3887.
43. **Sayle, R. A., and E. J. Miller-White.** 1995. RASMOL: biomolecular graphics for all. Trends Biochem. Sci. **20:**374.
44. **Shergill, J. K., C. L. Joannou, J. R. Mason, and R. Cammack.** 1995. Coordination of the Rieske-type [2Fe-2S] cluster of the terminal iron-sulfur protein of *Pseudomonas putida* benzene 1,2-dioxygenase, studied by one- and two-dimensional electron spin-echo envelope modulation spectroscopy. Biochemistry **34:**16533–16542.
45. **Singer, M., and P. Berg.** 1991. mRNA translation in prokaryotes, p. 167–173. *In* Genes and genomes: a changing perspective. University Sciences Books, Sausalito, Calif.
46. **Suen, W.-C., and D. T. Gibson.** 1993. Isolation and preliminary characterization of the subunits of the terminal component of naphthalene dioxygenase from *Pseudomonas putida* NCIB 9816–4. J. Bacteriol. **175:**5877–5881.
47. **Suenaga, H., M. Mitsuoka, Y. Ura, T. Watanabe, and K. Furukawa.** 2001. Directed evolution of biphenyl dioxygenase: emergence of enhanced degradation capacity for benzene, toluene, and alkyl benzenes. J. Bacteriol. **183:**5441–5444.
48. **Tan, H. M., and C. M. Cheong.** 1994. Substitution of the ISP alpha subunit of biphenyl dioxygenase from *Pseudomonas* results in a modification of the enzyme activity. Biochem. Biophys. Res. Commun. **204:**912–917.
49. **Tan, H.-M., and J. R. Mason.** 1990. Cloning and expression of the plasmid-encoded benzene dioxygenase genes from *Pseudomonas putida* ML2. FEMS Microbiol. Lett. **72:**259–264.
50. **Tan, H. M., H. Y. Tang, C. L. Joannou, N. H. Abdel-Wahab, and J. R. Mason.** 1993. The *Pseudomonas putida* Ml2 plasmid-encoded genes for benzene dioxygenase are unusual in codon usage and low in G+C content. Gene **130:**33–39.
51. **Wackett, L. P., L. D. Kwart, and D. T. Gibson.** 1988. Benzylic monooxygenation catalyzed by toluene dioxygenase from *Pseudomonas putida.* Biochemistry **27:**1360–1367.
52. **Wolfe, M. D., D. J. Altier, A. Stubna, C. V. Popescu, E. Munck, and J. D. Lipscomb.** 2002. Benzoate 1,2-dioxygenase from *Pseudomonas putida*: single turnover kinetics and regulation of a two-component Rieske dioxygenase. Biochemistry **41:**9611–9626.
53. **Wolfe, M. D., J. V. Parales, D. T. Gibson, and J. D. Lipscomb.** 2001. Single turnover chemistry and regulation of O-2 activation by the oxygenase component of naphthalene 1,2-dioxygenase. J. Biol. Chem. **276:**1945–1953.
54. **Yanisch-Perron, C., J. Vieira, and J. Messing.** 1985. Improved M13 phage cloning vectors and host strains: nucleotide sequences of the M13mp18 and Puc19 vectors. Gene **33:**103–119.
55. **Zamanian, M., and J. R. Mason.** 1987. Benzene dioxygenase in *Pseudomonas*

putida. Subunit composition and immuno-cross-reactivity with other aromatic dioxygenases. Biochem. J. **244:**611–616.

56. **Zhang, N., B. G. Stewart, J. C. Moore, R. L. Greasham, D. K. Robinson, B. C. Buckland, and C. Lee.** 2000. Directed evolution of toluene dioxygenase from *Pseudomonas putida* for improved selectivity towards cis-indandiol during indene bioconversion. Metab. Eng. **2:**339–348.
57. **Zylstra, G. J., and D. T. Gibson.** 1989. Toluene degradation by *Pseudomonas putida* F1: nucleotide sequence of the Todc1C2BADE genes and their expression in *Escherichia coli.* J. Biol. Chem. **264:**14940–14946.
58. **Zylstra, G. J., W. R. McCoombie, D. T. Gibson, and B. A. Finette.** 1988. Toluene degradation by *Pseudomonas putida* F1: genetic organization of the *tod* operon. Appl. Environ. Microbiol. **54:**1498–1503.